



ELSEVIER

Available online at www.sciencedirect.com

SCIENCE @ DIRECT®

Tetrahedron 62 (2006) 8467–8473

Tetrahedron

Two-photon absorption chromophores with a tunable [2,2']bithiophene core

Chia-Feng Chou,^{a,b} Tai-Hsiang Huang,^a Jiann T. Lin,^{a,*} Cheng-chih Hsieh,^c Chin-Hung Lai,^c Pi-Tai Chou^{c,*} and Chiutang Tsai^{b,*}

^a*Institute of Chemistry, Academia Sinica, Taipei 11529, Taiwan, ROC*

^b*Department of Chemistry, Chinese Culture University, Taipei 320, Taiwan, ROC*

^c*Department of Chemistry, The National Taiwan University, Taipei 106, Taiwan, ROC*

Received 15 May 2006; revised 22 June 2006; accepted 23 June 2006

Available online 17 July 2006

Abstract—Sonogashira coupling between 3,5,3',5'-tetrabromo-[2,2']bithiophene and various terminal alkynes provides two-photon absorption (TPA) chromophores **1–6**, which possess electron donor (D) and/or acceptor (A) alkynyl substituents at 3(3') and 5(5') sites of the bithiophene core. The up-converted fluorescence emission excited at 800 nm (Ti:sapphire femtosecond laser, ~100 fs pulses) was used to determine the two-photon absorption cross-sections (σ) of these compounds. The corresponding TPA cross-section (σ) values ranging from 132 to 1120 GM (10^{-50} cm⁴ s photon⁻¹) can be fine-tuned by the substituents. The quadrupolar-type (A- π -D- π -A) chromophore **5** exhibits the largest σ value (1120 GM) in CH₂Cl₂ upon 800 nm excitation.

© 2006 Elsevier Ltd. All rights reserved.

1. Introduction

The two-photon process involving simultaneous absorption (nonresonance–resonance) of two photons was first predicted by Goppert-Mayer in 1931,¹ and experimentally observed in the 1960s.² Two-photon absorption (TPA) offers the advantage of high transmission at low incident intensity for fundamental frequencies well below the band gap. Furthermore, due to the quadratic dependence of the two-photon absorption probability on intensity, the absorption can theoretically be confined to a volume of order λ^3 (where λ is the laser wavelength) under tight-focusing conditions. Therefore, one is able to initiate two-photon polymerization for three-dimensional optical data storage and microfabrication using near infrared (NIR) laser source.³ Another important application of TPA is confocal microscopy, which is an important tool for obtaining three-dimensional (3D) images of biological specimens such as tissues and cells.⁴ Two-photon confocal laser scanning microscopy has several advantages over its single-photon counterpart. Except for the depth resolution due to the quadratic dependence of the two-photon induced fluorescence intensity on the excitation power, the

NIR excitation light provides much better penetration ability compared to UV and even visible light in many organic materials where the linear attenuation and scattering are high.⁵ Other important applications of TPA chromophores include two-photon optical power-limiting,⁶ two-photon up-converted lasing,⁷ and photodynamic therapy.⁸

In light of above fundamental applications, significant progress has been made on the development of organic conjugated molecules with large TPA cross-sections.⁹ Among these, quadrupolar and octupolar-type molecules have received considerable interests because of the significant enhancement of the TPA cross-section in these molecules compared to their dipolar-type analogues.¹⁰ Further increment of TPA cross-section has been achieved by incorporating TPA chromophores in a dendrimer to increase the density of chromophores.¹¹ In their seminal report, Marder and Perry illustrated that molecules with a D- π -D, A- π -A, D- π -A- π -D or A- π -D- π -A motif (D = electron donor; A = electron acceptor; π = conjugated bridge) were potential quadrupolar-type TPA chromophores, which could exhibit exceptional large TPA cross-sections.¹² Based on previous studies,¹² it was concluded that TPA cross-sections were larger in molecules with more effective conjugation length and higher polarizability. Accordingly, coplanarity of the conjugation bridge is beneficial to the increase of the TPA cross-sections. Practically, for the biological application, it is advantageous to have the two-photon peak occurring at or near 800 nm where most of organic and biological

Keywords: Two-photon absorption; Bithiophene; Sonogashira coupling reaction.

* Corresponding authors. Tel.: +886 2 27898522; fax: +886 2 27831237 (J.T.L.); tel.: +886 2 33663893; fax: +886 2 23695208 (P.-T.C.); tel.: +886 2 28610511 376; fax: +886 2 28614212 (C.T.); e-mail addresses: jtlin@chem.sinica.edu.tw; chop@ntu.edu.tw; tsaictom@faculty.pccu.edu.tw

materials have large optical transparency. Also, there is a greater penetration depth in tissue with reduced photodamage upon ~ 800 nm excitation.

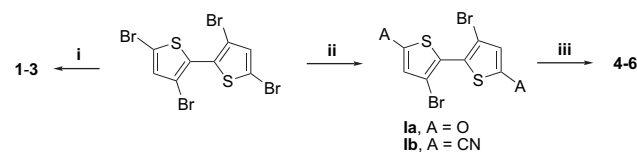
It is thus important to gain detailed insights into the relationship between molecular structure and TPA cross-section σ . The results may provide a guideline for future design and synthesis of organic molecules with highly efficient TPA. To achieve this goal, we have been interested in the systematic development of organic quadrupolar- or octupolar-type TPA chromophores.¹³ Herein, we report the investigations on the TPA properties of a series of novel quadrupolar chromophores based on 3,3',5,5'-tetrasubstituted-[2,2']-bithiophene core. In this approach, 3,5,3',5'-tetrabromo-[2,2']bithiophene¹⁴ was subjected to Sonogashira coupling reaction¹⁵ with terminal alkynes based on the following considerations: (1) the substituents introduced at the 3 and 3' sites can differ in the electronic property from those introduced at the 5 and 5' sites due to different reactivity of the 3(3') and 5(5') bromos and (2) incorporation of ethynyl entity in the conjugation chain normally results in less effective conjugation length.¹⁶ This strategic design may avoid shifting the one-photon absorption towards 800 nm, while the coplanarity of aromatic rings, especially the central [2,2']-bithiophene core, can be retained upon electronic tuning.

2. Results and discussion

2.1. Synthesis and characterization

Figure 1 depicts the structures of the new series of compounds **1–6**, and their corresponding synthetic routes are illustrated in Scheme 1. These compounds were synthesized via Sonogashira coupling¹⁵ of 3,5,3',5'-tetrabromo-[2,2']bithiophene and appropriate terminal alkynes catalyzed by 3 mol % of $\text{PdCl}_2(\text{PPh}_3)_2$ and CuI in diisopropylamine. Compounds **1–3**, in which all four bromine atoms in 3,5,3',5'-tetrabromo-[2,2']bithiophene are replaced by the same substituents, were isolated in good yields (**1**, 62%; **3**, 80%) except for **2** (20%) if slight excess of terminal alkynes

were used. Conversely, if only ~ 2 equiv of terminal alkynes were used and the reaction was allowed to proceed at lower temperature (40 °C), the Sonogashira coupling selectively occurred at the 5 and 5' sites to afford the dibromo intermediates (**1a** and **1b**) in moderate to good yields. This is consistent with the previous reports¹⁷ that the halo atom at the 2- or 5-site of halothiophene moieties was more reactive to undergo Sonogashira coupling reaction. These dibromo intermediates can subsequently undergo further Sonogashira coupling reactions with different terminal alkynes to afford **4–6** in 30–40% yields. Compounds **1–6** are moderately soluble in common solvents and have been characterized by ^1H and ^{13}C NMR and mass spectroscopic studies.



- i. 1.5 mol% $\text{PdCl}_2(\text{PPh}_3)_2$, 0.5 mol% CuI, 1.5 mol% PPh_3 , 4.4 equiv. terminal alkynes, *i*-Pr₂NH, rt 30 min., then reflux 2 days
- ii. 1.5 mol% $\text{PdCl}_2(\text{PPh}_3)_2$, 0.5 mol% CuI, 1.5 mol% PPh_3 , 2.2 equiv. terminal alkynes, *i*-Pr₂NH, rt 5 h, 40 °C 5 h, then reflux 1 day
- iii. 3 mol% $\text{PdCl}_2(\text{PPh}_3)_2$, 1 mol% CuI, 3 mol% PPh_3 , 2.2 equiv. terminal alkynes, *i*-Pr₂NH, rt 30 min., then reflux 2 days

Scheme 1.

2.2. Linear absorption and single-photon-excited fluorescence (SPEF)

Steady state absorption and emission spectra of the representative compound **5** are depicted in Figure 2, and the associated photophysical properties for **1–6** are listed in Table 1. The lower lying energy band ($\lambda_{\text{abs}}^{(1)} > 430$ nm) in compounds **1–3** is tentatively attributed to the π - π^* extending network through the substituents (A=O, N or T, see Fig. 1) and the [2,2']bithiophene core. Support of this viewpoint is given by the disappearance of this band upon replacing the 3- and 3'-substituents by the bromine atom. Furthermore, the substituent (O, N or T) alone exhibits the lowest absorption band of < 400 nm. For compounds **4–6**, in addition to the elongation of the conjugated π bonds, the lowest lying

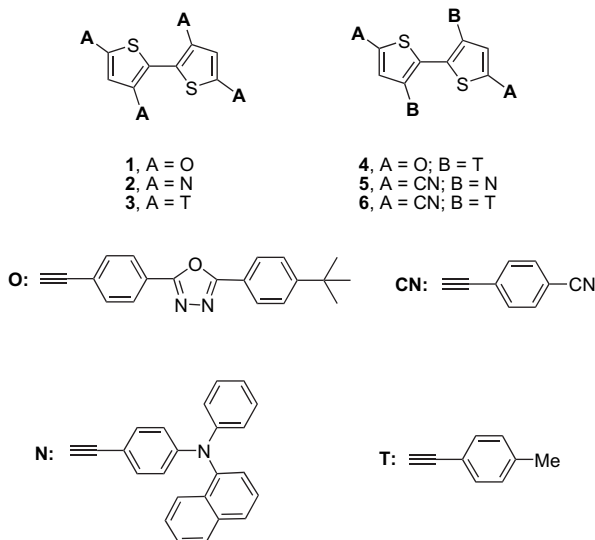


Figure 1. Molecular structures of compounds **1–6** and various alkyne moieties.

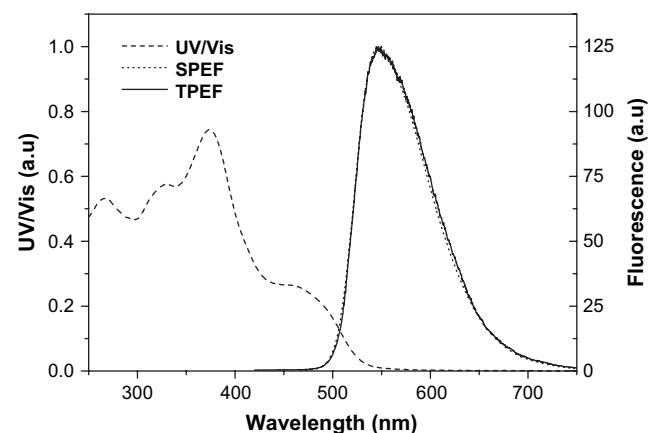


Figure 2. One-photon absorption (dashed line), single-photon-excited fluorescence (SPEF, $\lambda_{\text{ex}}=400$ nm), and two-photon excitation fluorescence (TPEF, $\lambda_{\text{ex}}=800$ nm) spectra of compound **5** in CH_2Cl_2 . (SPEF and TPEF are in dotted and solid lines, respectively).

Table 1. One- and two-photon properties of compounds **1–6** and references

Compounds	$\lambda_{\text{abs}}^{(1)\text{a}}$ (nm)	$\lambda_{\text{em}}^{(1)\text{b}}$ (nm)	$\Phi_{\text{f}}^{\text{c}}$	$\lambda_{\text{abs}}^{(2)\text{d}}$ (nm)	$\sigma^{\text{e,f,g}}$ (GM)
1	444,350,313,292	517	0.42	800	295 (0.22)
2	463,357,318,268	543	0.37	800	236 (0.16)
3	431,324,315,248	487	0.41	800	132 (0.21)
4	443,336,296	498	0.22	800	615 (0.62)
5	458,374,329	547	0.21	800	1120 (1.07)
6	440,333,253	492	0.10	800	665 (0.98)
C-480			0.87	800	168.2
R-6G			0.98	800	38.67

^a $\lambda_{\text{abs}}^{(1)}$ of the one-photon absorption spectra in nanometers.

^b $\lambda_{\text{em}}^{(1)}$ of the one-photon emission spectra in nanometers.

^c Fluorescence quantum yield.

^d $\lambda_{\text{abs}}^{(2)}$ of the two-photon absorption spectra in nanometers.

^e TPA cross-section in 10^{-50} cm⁴/s/photon (GM).

^f Numbers in the parenthesis are relative σ/MW .

^g Samples measured in CH₂Cl₂ at a concentration of 10^{-4} M, Coumarin 480 (**C-480**) and Rhodamine 6G (**R-6G**) measured in MeOH at a concentration of 10^{-4} M. Compounds **1**, **3**, and **4** compared to Coumarin 480; **2**, **5**, and **6** compared to Rhodamine 6G.

Table 2. The S₀–S₁ excitation energies and oscillation strengths of the twisted and planar **4** and **5** calculated with ZINDO//HF/3-21G* method

State	E_{cal} (eV)	λ_{cal} (nm)	f
4			
Twisted ^a			
S ₁	2.95	420	1.1298
Planar			
S ₁	2.51	493	1.0196
5			
Twisted ^b			
S ₁	2.95	420	0.7889
Planar			
S ₁	2.48	499	0.8650

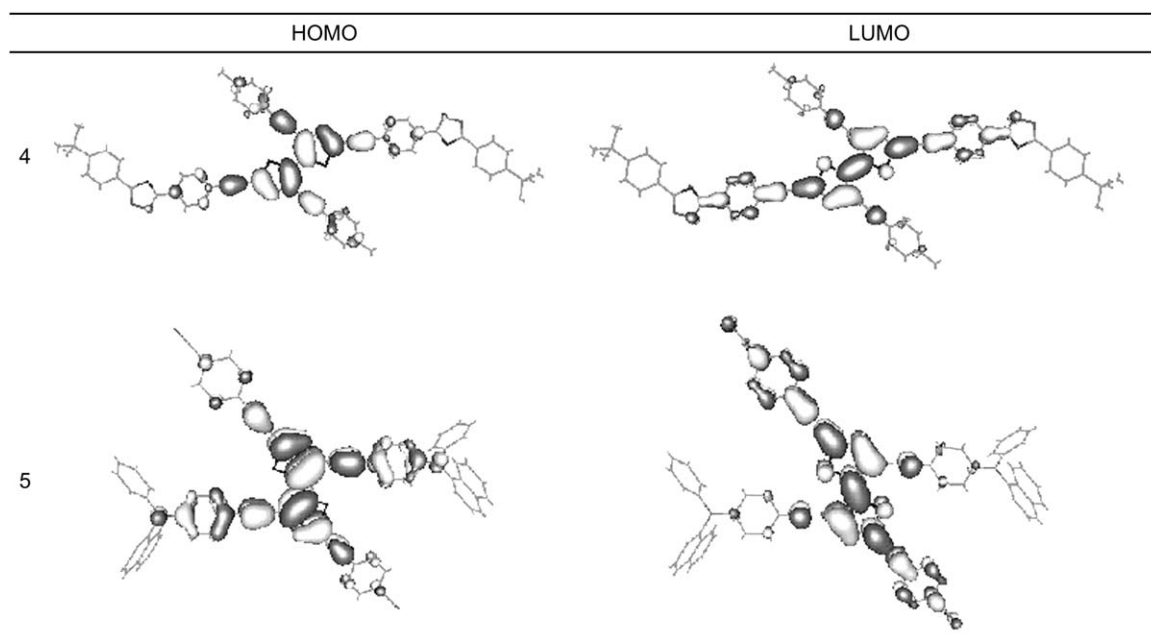
^a The dihedral angles of the twisted and planar forms are 56.28° and –179.9°, respectively.

^b The dihedral angles of the twisted and planar forms are –56.49° and 177.3°, respectively.

absorption band with $\lambda_{\text{abs}}^{(1)}$ above 440 nm, to a certain extent, may also possess a charge transfer character from the 3- (or 3'-) donor to the 5- (or 5'-) acceptor site bridged by [2,2']-bithiophene core. These assignments are supported by the theoretical approach on two prototypical compounds, **4** and **5** (see Table 2 and Fig. 3), in which, upon HOMO → LUMO transition in **5**, the electron density significantly decreases in electron donating group *N* (see Fig. 1 for definition), accompanied by the increase of the electron density in the electron accepting group *CN*.

2.3. TPA cross-sections

The up-converted fluorescence emission technique¹⁸ was used to determine the two-photon absorption cross-sections (σ) of the studied compounds. In order to eliminate contribution from the excited-state absorption, the femtosecond (~100 fs) pulsed laser was used for the measurement. The two well characterized TPA chromophores, Coumarin 480 (with a TPA cross-section value of 168.2 GM)^{19a} and Rhodamine 6G (with a TPA cross-section value of 38.67 GM),^{19b} were used as the references. TPA cross-sections of compounds **1–6** obtained from the two-photon excitation fluorescence (TPEF) are compiled in Table 1. For a clear comparison, the TPA cross-section per unit mass was also calculated and listed in Table 1. A prototypical TPEF spectrum of **5** is displayed in Figure 2, while the representative two-photon excitation (TPE) spectra (750–840 nm) of **5** and **6** in CH₂Cl₂ are displayed in Figure 4. Comparing TPE and single-photon absorption spectra for **5** and **6**, the TPE peak appears at an energy slightly higher than twice that of the corresponding linear absorption maximum, indicating a different selectivity of transition, in part, between one and two-photon absorption. Nevertheless, compounds **1–6** have nearly superimposable single-photon-excited fluorescence and TPEF spectra, supporting that both emissions originate from the same lowest lying transition in the singlet manifold.

**Figure 3.** The HOMO and LUMO of planar compounds **4** and **5**. Note that the first singlet excited state is dominated by the HOMO → LUMO transition.

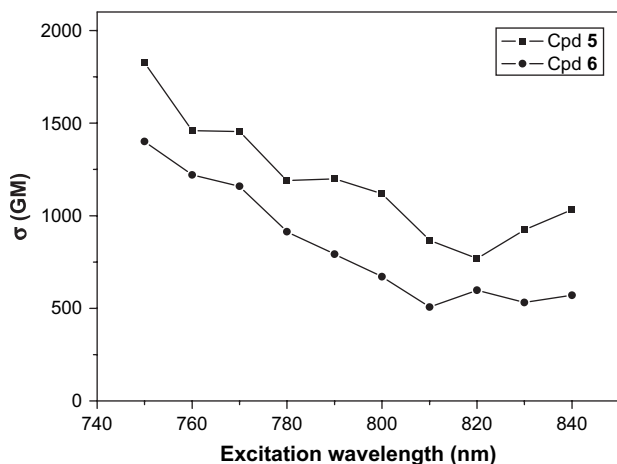


Figure 4. The two-photon excitation (TPE) spectra (750–840 nm) of **5** and **6** in CH_2Cl_2 .

According to the data, compound **4** has significantly higher TPA cross-section than that of **1**, though the latter seems to have a larger conjugation length. Qualitatively, if one considers thiophene and oxadiazole moieties to be π -excessive and π -deficient, respectively, the two peripheral oxadiazole-containing segments at the 5 and 5' positions together with the [2,2']bithiophene core constitute an A- π -D- π -A motif for TPA chromophore **4**. This consideration requires the coplanarity of the molecular structure. Though the PM3 method indicates that each compound (**1**–**6**) possesses a dominant twisted form, the thermodynamic properties of the twisted and planar forms in the ground state are nearly degenerate based on the ab initio (HF/3-21G*) calculation, i.e., energy difference ($E_{\text{planar}} - E_{\text{twisted}}$) are 0.3 and -0.05 kcal/mol for **4** and **5**, respectively. In addition, due to the negligible C(2)-C(2') rotation barrier there should exist a very fast equilibrium between these rotational isomers at room temperature. Upon excitation, the conversion from twisted to planar form should be fast and highly exothermic (see Table 2), such that the consequence is suited for a quadrupolar mechanism.

As such, the two tolyl-containing segments in **4** will enhance the electron donor character of the [2,2']bithiophene core, while the two oxadiazole-containing segments at the 3 and 3' positions (compound **1**) have an opposite effect. Likewise, both **5** and **6** also possess an A- π -D- π -A motif and the TPA cross-section of **5** is nearly 1.7 times as large as that of **6**. This trend can be attributed to a stronger π -donor for diarylamine (**5**) than that of the methyl group (**6**), resulting in an increase of σ value in **5**. Compound **6** has somewhat larger σ value than **4**, implying that the cyanophenyl moiety can lead to greater polarizability than the oxadiazole segment.

3. Conclusion

In summary, we have designed and synthesized a new series of [2,2']bithiophene-based quadrupolar-type chromophores exhibiting large TPA cross-sections. We also demonstrate that the incorporation of push and pull segments at the 3/3' and 5/5' sites with different arrangements significantly alter the corresponding TPA property. We thus believe that an

increment of the electron donor/acceptor strength in TPA chromophores with an A- π -D- π -A motif should enlarge the quadrupole moment and hence the TPA cross-section. On this basis, further fine-tuning of the TPA properties on [2,2']bithiophene-based chromophores should be feasible via the variation of the donor, acceptor as well as the conjugation chain. In view of applications, on the basis of the [2,2']bithiophene core, conversion of these compounds into polymers for the device fabrication is also feasible. This should greatly extend the usefulness of [2,2']bithiophene-based chromophores in the field of information storage, microfabrication, etc. Works focused on these issues are currently in progress.

4. Experimental

4.1. General procedures and spectroscopic measurements

Unless otherwise specified, all the reactions were carried out under nitrogen atmosphere using standard Schlenk techniques. Solvents were dried by standard procedures. All column chromatography was performed with the use of silica gel (230–400 mesh, Macherey–Nagel GmbH & Co.) as the stationary phase. The ^1H NMR spectra were recorded on a Bruker AMX400 spectrometer. Electronic absorption spectra were measured in various solvents using a Cary 50 Probe UV–visible spectrophotometer. Emission quantum yields were measured with reference to Coumarin 1 or 6 in CH_3CN .²⁰ Mass spectra (FAB) were recorded on a JMS-700 double focusing mass spectrometer (JEOL, Tokyo, Japan). Elementary analyses were performed on a Perkin–Elmer 2400 CHN analyzer. 2-Bromothiophene, sodium azide, bromobenzonitrile, 4-*tert*-butylbenzyl chloride, trimethylsilylacetylene, *N*-phenyl-1-naphthylamine, 4-ethynyl-toluene, *N,N*-diphenylamine, and hydrobromic acid were purchased from Acros. 1-Bromo-4-iodobenzene and Br_2 were purchased from Aldrich. Potassium hydroxide and magnesium sulfate were purchased from SOWA. The starting materials 3,5,3',5'-tetrabromo-[2,2']bithiophene,²¹ 2-(4-*tert*-butyl-phenyl)-5-(4-ethynyl-phenyl)-[1,3,4]oxadiazole,²² and (4-ethynyl-phenyl)-naphthalen-1-yl-phenyl-amine²³ were prepared according to the literature procedures with slight modifications.

4.2. General procedures for the synthesis of identical tetra-substituted compounds

Compounds 3,5,3',5'-tetrakis-2-(4-*tert*-butyl-phenyl)-5-(4-ethynyl-phenyl)-[1,3,4]oxadiazole-[2,2']bithiophene (**1**), 3,5,3',5'-tetrakis(4-ethynyl-phenyl)-naphthalenyl-phenylamine-[2,2']bithiophene (**2**), and 3,5,3',5'-tetrakis-*p*-tolylethynyl-[2,2']bithiophene (**3**) were synthesized by a similar procedure as the following description. To a flask containing 3,5,3',5'-tetrabromo-[2,2']bithiophene (1 equiv), $\text{PdCl}_2(\text{PPh}_3)_2$ (3 mmol % per bromo atom), CuI (1 mmol % per bromo atom), PPh_3 (3 mmol % per bromo atom), and aromatic acetylene (4.4 equiv per halogen atom) was added *i*- Pr_2NH (50 mL). The resulting mixture was stirred at room temperature for 30 min, allowed to reflux for two days. The solvent was removed under vacuum, and the residue was extracted with CH_2Cl_2 and brine. Removal of CH_2Cl_2 provided

a yellow residue, which was purified by column chromatography using THF/*n*-hexane as eluent and followed by recrystallization from CH₂Cl₂ and MeOH.

4.2.1. Compound (1). Orange solid, yield 62% (360 mg). Mp: 333–335 °C. IR (KBr): ν_{\max} 3055 w, 2930 w, 2130 w cm⁻¹. ¹H NMR (CDCl₃): δ 8.17–8.13 (m, 8H), 8.04 (d, *J*=7.8 Hz, 8H), 7.77 (d, *J*=8.0 Hz, 4H), 7.67 (d, *J*=7.8 Hz, 4H), 7.53 (d, *J*=8.0 Hz, 8H), 7.41 (s, 2H), 1.35 (s, 36H). ¹³C NMR (CDCl₃): δ 31.11, 35.11, 84.49, 87.74, 95.09, 96.05, 119.61, 120.87, 121.96, 123.90, 125.56, 126.10, 126.82, 126.90, 131.96, 132.03, 135.48, 139.06, 155.52, 155.57, 163.73, 164.90. FAB MS (*m/z*): 1367 (M⁺+H). HRMS Calcd for C₈₈H₇₁N₈O₄S₂: 1367.5040. Found: 1367.5033. Anal. Calcd for C₈₈H₇₀N₈O₄S₂: C, 77.28; H, 5.16; N, 8.19. Found: C, 76.90; H, 5.22; N, 8.01.

4.2.2. Compound (2). Orange solid, yield 20% (350 mg). Mp: 246 °C (decomp.). IR (KBr): ν_{\max} 3058 w, 2130 cm⁻¹. ¹H NMR (CDCl₃): δ 7.88 (t, *J*=9.6 Hz, 4H), 7.79 (t, *J*=9.0 Hz, 4H), 7.68–7.63 (m, 4H), 7.52–7.44 (m, 8H), 7.42–7.33 (m, 12H), 7.21–7.17 (m, 12H), 7.15 (s, 2H), 7.10 (t, *J*=6.7 Hz, 8H), 7.01 (t, *J*=7.6 Hz, 4H), 6.91–6.83 (m, 8H). ¹³C NMR (CDCl₃): δ 84.24, 86.67, 95.12, 96.49, 115.85, 117.36, 120.47, 121.78, 122.96, 125.65, 125.99, 126.08, 127.71, 128.28, 128.76, 129.32, 132.10, 132.96, 134.66, 138.72, 144.72. FABMS (*m/z*): 1434 (M⁺). HRMS Calcd for C₁₀₄H₆₆N₄S₂: 1434.4729. Found: 1434.4740. Anal. Calcd for C₁₀₄H₆₆N₄S₂: C, 87.00; H, 4.63; N, 3.90. Found: C, 87.11; H, 4.90; N, 3.82.

4.2.3. Compound (3). Yellow solid, yield 80% (1.02 g). Mp: 225–227 °C. IR (KBr): ν_{\max} 3055 w, 2930 w, 2130 w cm⁻¹. ¹H NMR (CDCl₃): δ 7.50 (s, *J*=8.1 Hz, 4H), 7.4 (s, *J*=8.0 Hz, 4H), 7.27 (s, 2H), 7.19 (d, *J*=7.9 Hz, 4H), 7.15 (d, *J*=8.0 Hz, 4H), 2.37 (s, 6H), 2.35 (s, 6H). ¹³C NMR (CDCl₃): δ 21.58, 81.50, 84.72, 92.62, 95.37, 96.61, 119.56, 119.97, 122.05, 129.19, 129.28, 131.42, 134.63, 138.08, 138.96. FABMS (*m/z*): 622 (M⁺). HRMS Calcd for C₄₄H₃₀S₂: 622.1789. Found: 622.1790. Anal. Calcd for C₄₄H₃₀S₂: C, 84.85; H, 4.85. Found: C, 84.47; H, 5.02.

4.3. General procedures for the synthesis of dibromo-substituted compounds

Compounds 3,3'-dibromo-5,5'-2-(4-*tert*-butyl-phenyl)-5-(4-ethynyl-phenyl)-[1,3,4]oxadiazole-[2,2']bithiophene (**1a**) and 4,4'-(3,3'-dibromo-2,2'-bithiophene-5,5'-diyl)bis(ethyne-2,1-diyl)dibenzonitrile (**1b**) were synthesized by a similar procedure as the following description. To a flask containing 3,5,3',5'-tetrabromo-[2,2']bithiophene (1 equiv), PdCl₂(PPh₃)₂ (1.5 mmol % per bromo atom), CuI (0.5 mmol % per bromo atom), PPh₃ (1.5 mmol % per bromo atom), and aromatic acetylene (2.2 equiv per halogen atom) was added *i*-Pr₂NH (70 mL). The resulting mixture was stirred at room temperature for 5 h, then heated to 40 °C for 5 h and allowed to reflux for one day. The solvent was removed under vacuum, and the residue was extracted with CH₂Cl₂ and brine. Removal of CH₂Cl₂ provided an orange residue, which was purified by column chromatography using THF/*n*-hexane as eluent and followed by recrystallization from CH₂Cl₂ and MeOH.

4.3.1. Compound (1a). Yellow solid, yield 25% (250 mg). Mp: 285 °C (decomp.). IR (KBr): ν_{\max} 3045 w, 2910 w, 2115 w cm⁻¹. ¹H NMR (CDCl₃): δ 8.13 (d, *J*=8.3 Hz, 4H), 8.05 (d, *J*=8.0 Hz, 4H), 7.66 (d, *J*=8.3 Hz, 4H), 7.54 (d, *J*=8.0 Hz, 4H), 7.27 (s, 2H), 1.36 (s, 18H). ¹³C NMR (CDCl₃): δ 31.10, 35.12, 86.52, 95.02, 97.10, 112.10, 112.85, 114.80, 125.45, 126.10, 126.29, 126.82, 128.29, 132.41, 132.98, 155.57. FABMS (*m/z*): 922 (M⁺). HRMS Calcd for C₄₈H₃₆Br₂N₄O₂S₂: 922.0646. Found: 922.0626. Anal. Calcd for C₄₈H₃₆Br₂N₄O₂S₂: C, 62.34; H, 3.92; N, 6.06. Found: C, 62.21; H, 3.87; N, 6.12.

4.3.2. Compound (1b). Yellow solid, yield 60% (840 mg). Mp: 253 °C (decomp.). IR (KBr): ν_{\max} 3046 w, 2200 w, 2120 cm⁻¹. ¹H NMR (CDCl₃): δ 7.61 (d, *J*=7.8 Hz, 4H), 7.51 (d, *J*=7.8 Hz, 4H), 7.02 (s, 2H). ¹³C NMR (CDCl₃): δ 90.57, 90.79, 111.20, 112.04, 114.76, 117.99, 127.96, 132.59, 132.93, 133.35. FABMS (*m/z*): 571 (M⁺). HRMS Calcd for C₂₆H₁₀Br₂N₂S₂: 571.8652. Found: 571.8632. Anal. Calcd for C₂₆H₁₀Br₂N₂S₂: C, 54.37; H, 1.76; N, 4.88. Found: C, 54.86; H, 1.72; N, 4.64.

4.4. General procedures for the synthesis of compounds 4–6

Compounds 3,3'-tetrakis-*p*-tolylethynyl-5,5'-2-(4-*tert*-butyl-phenyl)-5-(4-ethynyl-phenyl)-[1,3,4]oxadiazole-[2,2']bithiophene (**4**), 4,4'-(3,3'-bis((4-(naphthalen-1-yl(phenyl)amino)phenyl)ethynyl)-2,2'-bithiophene-5,5'-diyl)bis(ethyne-2,1-diyl)dibenzonitrile (**5**), and 4,4'-(3,3'-bis(*p*-tolylethynyl)-2,2'-bithiophene-5,5'-diyl)bis(ethyne-2,1-diyl)dibenzonitrile (**6**) were synthesized by a similar procedure as the following description. To a flask containing dibromocompounds (**1a** or **1b**) (1 equiv), PdCl₂(PPh₃)₂ (3 mmol % per bromo atom), CuI (1 mmol % per bromo atom), PPh₃ (3 mmol % per bromo atom), and aromatic acetylene (2.2 equiv per halogen atom) was added *i*-Pr₂NH (100 mL). The resulting mixture was stirred at room temperature for 30 min, allowed to reflux for two days. The solvent was removed under vacuum, and the residue was extracted with CH₂Cl₂ and brine. Removal of CH₂Cl₂ provided an orange-red residue, which was purified by column chromatography using THF/*n*-hexane as eluent and followed by recrystallization from CH₂Cl₂ and MeOH.

4.4.1. Compound (4). Orange solid, yield 30% (113 mg). Mp: 325 °C (decomp.). IR (KBr): ν_{\max} 3055 w, 2930 w, 2130 w cm⁻¹. ¹H NMR (CDCl₃): δ 8.02 (d, *J*=8.0 Hz, 4H), 8.01 (d, *J*=7.8 Hz, 4H), 7.68 (d, *J*=7.6 Hz, 4H), 7.64 (d, *J*=8.0 Hz, 4H), 7.52 (d, *J*=7.8 Hz, 4H), 7.24 (d, *J*=7.6 Hz, 4H), 7.00 (s, 2H), 2.41 (s, 6H), 1.35 (s, 18H). ¹³C NMR (CDCl₃): δ 21.42, 31.08, 35.08, 85.76, 89.14, 95.01, 97.41, 112.06, 114.78, 120.85, 125.27, 126.08, 126.27, 126.80, 128.19, 128.26, 129.00, 132.96, 137.81, 155.53. FABMS (*m/z*): 995 (M⁺+H). HRMS Calcd for C₆₆H₅₁N₄O₂S₂: 995.3453. Found: 995.3455. Anal. Calcd for C₆₆H₅₀N₄O₂S₂: C, 79.65; H, 5.06; N, 5.63. Found: C, 79.90; H, 5.11; N, 5.81.

4.4.2. Compound (5). Orange solid, yield 40% (226 mg). Mp: 242 °C (decomp.). IR (KBr): ν_{\max} 3055 w, 2200 w, 2150 w cm⁻¹. ¹H NMR (CDCl₃): δ 7.89 (dd, *J*=3.1, 8.2 Hz, 4H), 7.80 (d, *J*=8.2 Hz, 2H), 7.58 (d, *J*=8.0 Hz,

4H), 7.51 (d, $J=8.0$ Hz, 4H), 7.49–7.44 (m, 4H), 7.41–7.33 (m, 8H), 7.31 (s, 2H), 7.25–7.21 (m, 4H), 7.13 (d, $J=7.2$ Hz, 4H), 7.02 (t, $J=7.2$ Hz, 2H), 6.91 (d, $J=8.4$ Hz, 4H). ^{13}C NMR (CDCl_3): δ 87.51, 92.24, 94.08, 94.10, 111.41, 112.24, 114.91, 115.50, 118.18, 122.82, 123.39, 123.90, 124.30, 124.55, 124.75, 125.25, 125.54, 128.16, 129.35, 129.53, 129.70, 132.29, 132.49, 132.79, 133.14, 133.56, 147.15, 147.50. FABMS (m/z): 1050 (M^+). HRMS Calcd for $\text{C}_{74}\text{H}_{42}\text{N}_4\text{S}_2$: 1050.2851. Found: 1050.2858. Anal. Calcd for $\text{C}_{74}\text{H}_{42}\text{N}_4\text{S}_2$: C, 84.54; H, 4.03; N, 5.33. Found: C, 84.64; H, 4.31; N, 5.34.

4.4.3. Compound (6). Orange solid, yield 26% (80 mg). Mp: 282 °C (decomp.). IR (KBr): ν_{max} 3055 w, 2920 w, 2230 w, 2150 w cm^{-1} . ^1H NMR (CDCl_3): δ 7.63 (d, $J=8.8$ Hz, 4H), 7.57 (d, $J=8.8$ Hz, 4H), 7.50 (d, $J=8.0$ Hz, 4H), 7.36 (s, 2H), 7.21 (d, $J=8.0$ Hz, 4H), 2.39 (s, 6H). ^{13}C NMR (CDCl_3): δ 21.39, 81.52, 81.80, 112.24, 114.74, 118.18, 125.23, 126.90, 128.16, 128.94, 128.96, 131.95, 132.59, 132.91, 137.78. FABMS (m/z): 644 (M^+). HRMS Calcd for $\text{C}_{44}\text{H}_{24}\text{N}_2\text{S}_2$: 644.1381. Found: 644.1374. Anal. Calcd for $\text{C}_{44}\text{H}_{24}\text{N}_2\text{S}_2$: C, 81.96; H, 3.75; N, 4.34. Found: C, 82.10; H, 3.51; N, 4.61.

4.5. Measurement of two-photon cross-section by the two-photon-induced fluorescence method

The setup for TPEF excitation spectra and TPEF excitation cross-section measurement has been described in our previous report.^{13a} In brief, a femtosecond mode-locked Ti:sapphire laser (Spectra Physics) generates ~ 100 fs pulses at repetition rate of 82 MHz with an average power of 300–400 mW. The laser beam was focused on a sample cell (1 cm) by a lens with the focal length 6 cm. To minimize the effects of re-absorption, the excitation beam was focused as close as possible to the wall of the quartz cell, which faced the slit of the imaging spectrograph. TPEF was detected at a direction perpendicular to the pump beam. The TPEF was focused by a lens with the focal length 8 cm, and was coupled via an optical fiber (Acton, ILG-45-20-3) into an optical spectrum analyzer. Our optical spectrum analyzer consists of a CCD with detector control (ICCD-576G, Princeton Instruments, Inc.) in conjunction with a monochromator (SpectraPro-275, Acton Research Corporation) was used as a recorder.

The TPA and TPEF cross-sections (σ and σ_e , respectively) are basic parameters to evaluate a material's TPA and TPEF properties. From TPEF intensity data, σ_e and σ can be evaluated by using Eqs. 1 and 2,^{19a,24} expressed as, where r stands for the reference compound, n for the refractive index of solvents applied, and F for the integrated fluorescence intensity; the concentration of the molecules in solution was denoted as C .

$$\sigma_e = \sigma_{e,r} \frac{F n_r C_r}{F_r n C} \quad (1)$$

$$\sigma \Phi = \sigma_e \quad (2)$$

The TPEF cross-section σ_e is supposed to be linearly dependent on the TPA cross-section (σ) with the TPEF quantum

yield Φ' as the coefficient.^{19a} In most reports, the SPEF quantum yield Φ was adopted instead of Φ' , because Φ' is difficult to be measured. By referencing the TPEF cross-section of Coumarin 480 to be 146.3 GM (1 GM = 10^{-50} cm^4 s/photon)^{19a} and Rhodamine 6G to be 37.90 GM (1 GM = 10^{-50} cm^4 s/photon).^{19b} The TPA cross-sections of these compounds were obtained (Table 1). The TPEF spectra of all these compounds were taken when they were excited at 800 nm in CH_2Cl_2 . The TPEF of Coumarin 480 or Rhodamine 6G was measured as a standard under the same experimental conditions. We obtained the relative TPEF cross-sections σ_e of these compounds by comparing their TPEF to that of Coumarin 480 (compounds **1**, **3**, and **4**) or Rhodamine 6G (compounds **2**, **5**, and **6**) under exactly the same experimental conditions.

4.6. Theoretical calculation

All calculations are done with the Gaussian 03 program.²⁵ Hartree Fock is used with the basis set 3-21G* (hereafter designated as B3LYP).²⁶ The calculated minima have been carefully checked by frequency analyses to examine whether the number of the imaginary frequency is zero. Note that molecules considered here are large enough to preclude the use of ab initio methods with large basis sets. Alternatively, the electronic properties and UV–visible spectra (single-point calculation) were calculated with the ZINDO/S-CI method on the optimized structures.²⁷

Acknowledgements

This work is partially supported by the Institute of Chemistry, Academia Sinica, Department of Chemistry, National Taiwan University, and Department of Chemistry, Chinese Culture University.

References and notes

- Goppert-Mayer, M. *Ann. Phys.* **1931**, *9*, 273.
- (a) Rentzepis, P. M.; Pao, Y. H. *App. Phys. Lett.* **1964**, *156*, 964; (b) Peticolas, W. L. *Annu. Rev. Phys. Chem.* **1967**, *18*, 233; (c) McClain, W. M. *Acc. Chem. Res.* **1974**, *7*, 129; (d) Birge, R. R.; Pierce, B. M. *J. Chem. Phys.* **1979**, *70*, 165.
- Cumpston, B. H.; Ananthavel, S. P.; Barlow, S.; Dyer, D. L.; Ehrlich, J. E.; Erskine, L. L.; Heikal, A. A.; Kuebler, S. M.; Lee, I.-Y. S.; McCord-Maughon, D.; Qin, J.; Röckel, H.; Rumi, M.; Wu, X.-L.; Marder, S. R.; Perry, J. W. *Nature* **1999**, *398*, 51.
- (a) Carlsson, K.; Daniilsson, P. E.; Lenz, P. E.; Lijeborg, A.; Majlof, L.; Aslund, N. *Opt. Lett.* **1985**, *10*, 53; (b) White, J. G.; Amos, W. B.; Fordham, M. *J. Cell Biol.* **1987**, *105*, 41.
- Bhawalker, J. D.; Swiatkiewicz, J.; Prasad, P. N.; Pan, S. J.; Shih, A.; Samarabandu, J. K.; Cheng, P. C.; Reinhardt, B. A. *Polymer* **1997**, *17*, 4551.
- (a) Ehrlich, J. E.; Wu, X. L.; Lee, I.-Y.; Hu, Z.-Y.; Röckel, S. R.; Marder, S. R.; Perry, J. W. *Opt.* **1997**, *22*, 1843; (b) He, G. S.; Yuan, X.; Bhawakar, J. D.; Prasad, P. N. *Appl. Opt.* **1997**, *36*, 3387.
- (a) Bauer, C.; Schnabel, B.; Kley, E. B.; Scherf, U.; Giessen, H.; Mahr, R. *Adv. Mater.* **2002**, *14*, 673; (b) Jordan, G.; Kobayashi, T.; Blau, W. J.; Pfeiffer, S.; Hörhold, H. H. *Adv. Funct. Mater.* **2003**, *13*, 751.

8. (a) Frederiksen, P. K.; Jørgensen, M.; Ogiyby, P. R. *J. Am. Chem. Soc.* **2001**, *123*, 1215; (b) Frederiksen, P. K.; McIlroy, S. P.; Nielsen, C. B.; Nikolajsen, L.; Skovsen, E.; Jørgensen, M.; Mikkelsen, K. V.; Ogiyby, P. R. *J. Am. Chem. Soc.* **2005**, *127*, 255.
9. Marder, S. R. *Chem. Commun.* **2006**, 131.
10. (a) Macak, P.; Luo, Y.; Norman, H.; Ågren, H. *J. Chem. Phys.* **2000**, *113*, 7055; (b) Yang, W. J.; Kim, D. Y.; Kim, C. H.; Jeong, M. Y.; Jeon, S.-J.; Cho, B. R. *Org. Lett.* **2004**, *6*, 1389; (c) Yang, W. J.; Kim, D. Y.; Jeong, M. Y.; Kim, H. M.; Lee, Y. K.; Fang, X.; Jeon, S. J.; Cho, B. R. *Chem.—Eur. J.* **2005**, *11*, 4191; (d) Yoo, J.; Yang, S. K.; Jeong, M.-Y.; Ahn, H. C.; Jeon, S. J.; Cho, B. R. *Org. Lett.* **2003**, *5*, 645; (e) Yang, W. J.; Kim, C. H.; Jeong, M.-Y.; Lee, S. K.; Piao, M. J.; Jeon, S.-J.; Cho, B. R. *Chem. Mater.* **2004**, *16*, 2783.
11. Adronov, A.; Fréchet, J. M. J.; He, G. S.; Kim, K.-S.; Chung, S.-J.; Swiatkiewicz, J.; Prasad, P. N. *Chem. Mater.* **2000**, *12*, 2838.
12. Albota, M.; Beljonne, D.; Brédas, J.-L.; Ehrlich, J. E.; Fu, J.-Y.; Heikal, A. A.; Hess, S. E.; Kogej, T.; Levin, M. D.; Marder, S. R.; McCord-Maughon, D.; Perry, J. W.; Röckel, H.; Rumi, M.; Subramanian, G.; Webb, W. W.; Wu, X.-L.; Xu, C. *Science* **1998**, *281*, 1653.
13. (a) Huang, P.-H.; Shen, J.-Y.; Pu, S.-C.; Wen, Y.-S.; Lin, J. T.; Chou, P.-T.; Yeh, M.-C. *P. J. Mater. Chem.* **2006**, *16*, 850; (b) Liu, S.; Lin, K. S.; Churikov, V. M.; Su, Y. Z.; Lin, J. T.; Huang, T.-H.; Hsu, C. C. *Chem. Phys. Lett.* **2004**, *390*, 433.
14. Meng, H.; Huang, W. *J. Org. Chem.* **2000**, *65*, 3894.
15. Sonogashira, K.; Tohda, Y.; Hagihara, N. *Tetrahedron. Lett.* **1975**, 4467.
16. (a) Stiegman, A. E.; Graham, E.; Perry, K. J.; Khundker, L. R.; Chen, L. T.; Perry, J. W. *J. Am. Chem. Soc.* **1991**, *113*, 7658; (b) Cheng, L. T.; Tam, W.; Stevenson, S. H.; Meredith, G. R.; Rikken, G.; Marder, S. R. *J. Chem. Phys.* **1991**, *95*, 10631.
17. (a) Neenan, T. X.; Whitesides, G. M. *J. Org. Chem.* **1988**, *53*, 2489; (b) Solooki, D.; Kennedy, V. O.; Tessier, C. A.; Youngs, W. T. *Synlett* **1990**, 427; (c) Dahlmann, U.; Neidlein, R. *Helv. Chim. Acta* **1996**, *79*, 755.
18. Reinhardt, B. A.; Brott, L. L.; Clarson, S. J.; Dillard, A. G.; Bhatt, J. C.; Kannan, R.; Yuan, L.; He, G. S.; Prasad, P. N. *Chem. Mater.* **1998**, *10*, 1863.
19. (a) Albota, M. A.; Xu, C.; Webb, W. W. *Appl. Opt.* **1998**, *37*, 7352; (b) Fisher, W. G.; Wachter, E. A.; Lytle, F. E.; Armasand, M.; Seaton, C. *Appl. Spectrosc.* **1998**, *52*, 536.
20. Jones, G., II; Jackson, W. R.; Choi, C.-y.; Bergmark, W. R. *J. Phys. Chem.* **1985**, *89*, 294.
21. Inaoka, S.; Collard, D. M. *J. Mater. Chem.* **1999**, *9*, 1719.
22. Cha, S. E.; Choi, S.-H.; Kim, K.; Jin, J., II. *J. Mater. Chem.* **2003**, *13*, 1900.
23. Plater, M. J.; Jackson, T. *Tetrahedron* **2003**, *59*, 4687.
24. Xu, C.; Webb, W. W. *J. Opt. Soc. Am. B* **1996**, *13*, 481.
25. Frisch, M. J.; Trucks, G. W.; Schlegel, H. B.; Scuseria, G. E.; Robb, M. A.; Cheeseman, J. R.; Montgomery, J. A., Jr.; Vreven, T.; Kudin, K. N.; Burant, J. C.; Millam, J. M.; Iyengar, S. S.; Tomasi, J.; Barone, V.; Mennucci, B.; Cossi, M.; Scalmani, G.; Rega, N.; Petersson, G. A.; Nakatsuji, H.; Hada, M.; Ehara, M.; Toyota, K.; Fukuda, R.; Hasegawa, J.; Ishida, M.; Nakajima, T.; Honda, Y.; Kitao, O.; Nakai, H.; Klene, M.; Li, X.; Knox, J. E.; Hratchian, H. P.; Cross, J. B.; Adamo, C.; Jaramillo, J.; Gomperts, R.; Stratmann, R. E.; Yazyev, O.; Austin, A. J.; Cammi, R.; Pomelli, C.; Ochterski, J. W.; Ayala, P. Y.; Morokuma, K.; Voth, G. A.; Salvador, P.; Dannenberg, J. J.; Zakrzewski, V. G.; Dapprich, S.; Daniels, A. D.; Strain, M. C.; Farkas, O.; Malick, D. K.; Rabuck, A. D.; Raghavachari, K.; Foresman, J. B.; Ortiz, J. V.; Cui, Q.; Baboul, A. G.; Clifford, S.; Cioslowski, J.; Stefanov, B. B.; Liu, G.; Liashenko, A.; Piskorz, P.; Komaromi, I.; Martin, R. L.; Fox, D. J.; Keith, T.; Al-Laham, M. A.; Peng, C. Y.; Nanayakkara, A.; Challacombe, M.; Gill, P. M. W.; Johnson, B.; Chen, W.; Wong, M. W.; Gonzalez, C.; Pople, J. A. *Gaussian 03, Revision C.02*; Gaussian: Wallingford, CT, 2004.
26. Binkley, J. S.; Pople, J. A.; Hehre, W. J. *J. Am. Chem. Soc.* **1980**, *102*, 939.
27. Thompson, M. A.; Zerner, M. C. *J. Am. Chem. Soc.* **1991**, *113*, 8210.